A method to eliminate the influence of incident light variations in spectral analysis

Yongshun Luo,[1,2] Gang Li,[1,3] Zhigang Fu,[4] Yang Guan,[4] Shengzhao Zhang,[1,3] and Ling Lin[1,3,a)]

[1]*State Key Laboratory of Precision Measurement Technology and Instruments, Tianjin University, Tianjin 300072, China*
[2]*College of Mechanical and Electronic Engineering, Guangdong Polytechnic Normal University, Guangzhou 510635, China*
[3]*Tianjin Key Laboratory of Biomedical Detecting Techniques and Instruments, Tianjin University, Tianjin 300072, China*
[4]*Medical Examination Centre, No. 254 Hospital of PLA, Tianjin 300142, China*

(Received 13 February 2018; accepted 14 May 2018; published online 5 June 2018)

The intensity of the light source and consistency of the spectrum are the most important factors influencing the accuracy in quantitative spectrometric analysis. An efficient "measuring in layer" method was proposed in this paper to limit the influence of inconsistencies in the intensity and spectrum of the light source. In order to verify the effectiveness of this method, a light source with a variable intensity and spectrum was designed according to Planck's law and Wien's displacement law. Intra-lipid samples with 12 different concentrations were prepared and divided into modeling sets and prediction sets according to different incident lights and solution concentrations. The spectra of each sample were measured with five different light intensities. The experimental results showed that the proposed method was effective in eliminating the influence caused by incident light changes and was more effective than normalized processing. *Published by AIP Publishing.* https://doi.org/10.1063/1.5025768

I. INTRODUCTION

Quantitative near-infrared (NIR) spectrometric analysis is a nondestructive, pollution-free, simple, and convenient measurement method. It is widely used in the medical diagnosis,[1,2] characterization of foodstuff,[3–6] and analysis of factors in industries[7,8] and has a wide range of application prospects in the future. Since spectral analysis is an indirect measurement, the correlation model between the validation sets and the prediction sets depends heavily on the consistency of the incident light. The consistency and stability of the incident light are essential conditions for ensuring high accuracy and precision of measurements, which are essential in NIR spectrometric analysis.

There are two main factors that cause the variations of the incident light. One is the difference in incident light between the measurement system and the modeling system, which is mainly caused by the difference in light sources,[9] instrument installation errors,[10] and pathlength errors.[11] Another factor is the inconsistency of the light source due to the instability of power supply voltage[12] and bulb aging.[13] Many methods have been designed to keep the incident light consistent.

The common methods include the calibration of the incident light by several techniques, such as using standard reagents,[14] using auxiliary instruments,[15] and installing light intensity controllers.[12,13] The precision can also be further improved by modifying the model with calibration factors. However, accurate calibration is a complicated process, and many new errors can be generated during the calibration process,[16] such as the assembling errors generated from the installation of special optical fibers and spectroscopic instruments. The use of calibration instruments also increases the measurement cost and the operation time. In addition, when the measurement environment is changed, the error generated in the calibration process would be transformed. To eliminate the new errors would require further time and expenses. Due to the high cost and complexity of these calibration methods, they are not widely used in measurements. Moreover, inconsistencies in incident light can be generated by the instability of the light source.

High performance light sources[17] are used because they can provide high stability light with less probability of incident light changes. However, the inconsistency of the incident light generated by the differences between the measurement system and the modeling system cannot be avoided. The influence of incident light changes can be restrained by pretreatment methods, such as normalization.[18] However, the normalization processing is often used to eliminate the homogenization error. The variation of the incident spectra is difficult to predict, and attempts to eliminate its influence by calibration and using high performance instruments have limited effects. In general, after calibration and preprocessing, the incident light is regarded as constant, and the transmittance spectra or their logarithms are used as modeling samples.[19,20] This is known as the transmittance spectra method (TS method). The models are built based on the relationship between the transmittance spectra and the concentrations of components. Due to the absence of the incident light component in the model, systematic errors caused by the changes in intensity and wave band of the incident light cannot be eliminated. Therefore, it is difficult to improve the prediction accuracy of the model and, hence, to improve the robustness of the TS method. New measurement

a)Author to whom correspondence should be addressed: linling@tju.edu.cn

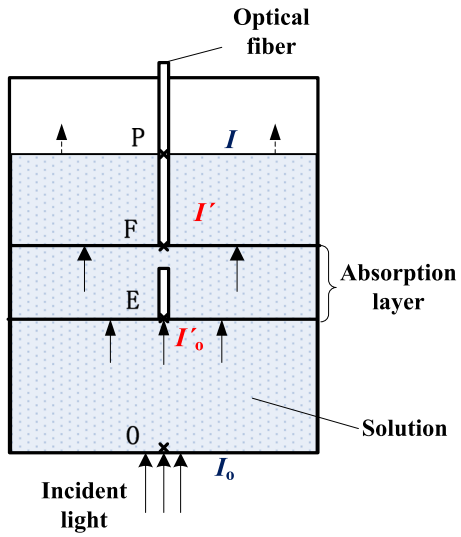

FIG. 1. Measurement positions of transmittance spectra in the ML method. Position O is the position of the original incident light. Position E is the measurement position of the incident light in the absorption layer. Position F is the measurement position of the transmitted light in the absorption layer. Position P is the position of the original transmitted light. Distance between positions E and F is the absorption layer.

methods need to be designed when the measurement system cannot be further improved.

The method of measuring in layer (ML method) is proposed in this study to eliminate the influence of the incident light variation. A thin liquid layer was selected as the absorption layer, and its incident light and the transmitted light were measured at the incident position and the transmittance position, respectively. The ML method was designed to address the difficulties in measuring the original incident light. The variation of the incident light was simulated by changing the intensity of the incident light in the experiments. The changes in the prediction accuracy were observed, and the feasibility of the ML method was verified. According to Planck's law and Wien's displacement law, the temperature of the filament will change when the voltage of the filament is changed, and the spectrum (including the intensity and frequency) of the light source will change accordingly. Therefore, the spectrum of the incident light source can be changed by changing the source voltage. Finally, the effectiveness of the normalization preprocessing of incident light variation was evaluated.

II. THEORETICAL BASIS AND METHOD

As shown in Fig. 1, the light source is placed under the container. The incident light (I_0) transmits through the solution and is fed into the spectrometer through the optical fiber (as shown in Fig. 2). Points O and P are the center points of the solution surface and are the incident point of light and the transmittance point of light, respectively. Lambert-Beer's law is the theoretical basis of spectral analysis. Based on this law, the relation between the absorbance and concentration is

$$A = \ln\left(\frac{I_0}{I}\right) = \varepsilon bc, \tag{1}$$

where A is the absorbance, I_0 is the incident light intensity measured at point O, I is the transmitted light intensity measured at point P, ε is the molar absorption coefficient, b is the pathlength which is the distance between points O and P, and c is the molar concentration. In general, I and I_0 are the intensities of the entire pathlength (for example, the distance between points O and P).

Due to the reflection of the light on the liquid surface, the scattering near the incident surface is serious, and the transmittance spectrum is severely affected by the scattering. With the increase in distance between the measurement position and the incident surface of the solution, the influence of the reflected light becomes weaker, the scattering becomes more uniform, and the nonlinearity reduces. Therefore, a position at a certain distance from the incident surface of the solution is suitable for measurement. Additionally, a thin layer is selected as the absorption layer. When the absorption layer is sufficiently thin, the scattering phenomenon is weak, and linearity becomes dominant. The case of Fig. 1 is taken as an example to illustrate the ideal distance measured in transmittance spectral analysis.

As shown in Fig. 1, point E is the measurement position of the incident light, and point F is the measurement position of the transmitted light. The light was measured by an optical fiber which was dipped in the solution. The liquid

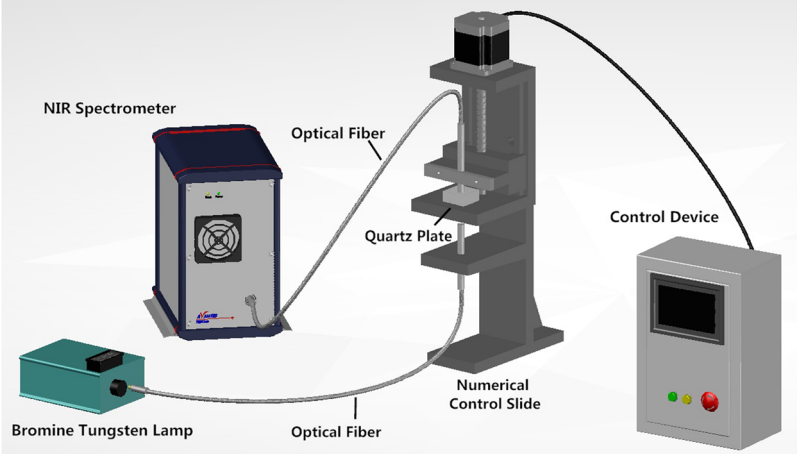

FIG. 2. Schematic diagram of light source interference measurement.

layer between points E and F is the absorption layer. In the ideal measurement condition, the distance between positions E and F is smaller than the distance between positions O and E. According to this rule, the nonlinear influence of incident light changes on the model can be reduced by the ML method in measurement. The absorbance of the absorption layer can be calculated approximately as follows:

$$A' = \ln(\frac{I'_o}{I'}) = \varepsilon b' c, \tag{2}$$

where A' is the absorbance of the absorption layer, b' is the pathlength of the absorption layer which is the distance between positions E and F, I'_o is the incident intensity of the absorption layer measured at position E, and I' is the transmittance intensity of the absorption layer measured at position F.

III. EXPERIMENT

An adjustable light source was used to provide different light intensities by accurately changing its voltage. The optical fiber was positioned accurately on the numerical control sliding table and was placed into the solution. The spectral data measured at two positions were received and recorded by the spectrometer.

A. Experimental setup

The experimental setup is shown in Fig. 2. An adjustable bromine tungsten lamp with a sensitivity of 1 mV was employed as the light source. The number of voltages tested was five (5.6 V, 5.9 V, 6.2 V, 6.5 V, and 6.8 V). All NIR spectra were measured from 1000 nm to 2500 nm by an AvaSpec-NIR256-2.5 (TEC) near-infrared spectrometer (Avates, Apeldoorn, The Netherlands). The solution was packed in a quartz plate of dimensions 18*18*16 mm. The optical fiber was fixed on the numerical control slide and was inserted into the solution. The slide was controlled by a numerical controller, and its kinematic accuracy was 0.01 mm. The NIR spectra were collected by the Avasoft7.6 software. In order to avoid the interference of the ambient light, the experimental setup was covered by a box wrapped with opaque black cloth.

B. Materials

Intra-lipid 30% suspension (Huarui Pharmaceutical Co., China) was the initial solution sample, and 11 other solutions were prepared by diluting the initial solution with distilled water. The resulting contents of intra-lipid in the 12 solutions were 30%, 28%, 26%, 24%, 22%, 20%, 18%, 16%, 14%, 12%, 10%, and 8%. The intra-lipid solutions have properties of strong light scattering, and scattering is sensitive to the change in light intensity.

C. Measurement

According to Planck's law and Wien's displacement law, the temperature of the filament changes when the voltage changes, and the spectrum of the light source (including the intensity and spectrum) changes accordingly. Therefore, the spectra of the incident light were modified by adjusting the source voltage. The first incident light (L1), second incident light (L2), third incident light (L3), fourth incident light (L4), and fifth incident light (L5) were emitted at the voltages of 5.6 V, 5.9 V, 6.2 V, 6.5 V, and 6.8 V, respectively.

The light source was 2 mm away from the plate bottom, and the optical fiber was inserted into the solution (as shown in Fig. 2). The spectra were digitalized with ca. 3 nm interval, resulting in 256 data points. Each sample was scanned for 350 ms, and the spectra from nine measurements were added for analysis. Position E was at 9 mm distance from the bottom of the quartz plate, and the length of the absorption layer was 3.5 mm.

To make the description more convenient, the light intensity and the absorbance are represented by the following symbols:

$$I^E_{i,j} = \begin{Bmatrix} I^E_{1,1} & I^E_{1,2} & \cdots & I^E_{1,11} & I^E_{1,12} \\ I^E_{2,1} & I^E_{2,2} & \cdots & I^E_{2,11} & I^E_{2,12} \\ I^E_{3,1} & I^E_{3,2} & \cdots & I^E_{3,11} & I^E_{3,12} \\ I^E_{4,1} & I^E_{4,2} & \cdots & I^E_{4,11} & I^E_{4,12} \\ I^E_{5,1} & I^E_{5,2} & \cdots & I^E_{5,11} & I^E_{5,12} \end{Bmatrix}, \quad I^F_{i,j} = \begin{Bmatrix} I^F_{1,1} & I^F_{1,2} & \cdots & I^F_{1,11} & I^F_{1,12} \\ I^F_{2,1} & I^F_{2,2} & \cdots & I^F_{2,11} & I^F_{2,12} \\ I^F_{3,1} & I^F_{3,2} & \cdots & I^F_{3,11} & I^F_{3,12} \\ I^F_{4,1} & I^F_{4,2} & \cdots & I^F_{4,11} & I^F_{4,12} \\ I^F_{5,1} & I^F_{5,2} & \cdots & I^F_{5,11} & I^F_{5,12} \end{Bmatrix}, \quad A_{i,j} = \ln(I^E_{i,j}/I^F_{i,j}), \tag{3}$$

where i is one of the five light intensity conditions (L1, L2, L3, L4, L5), j is the concentration, $I^E_{i,j}$ is the light intensity measured at position E, $I^F_{i,j}$ is the light intensity measured at position F, and $A_{i,j}$ is the absorbance.

The absorbance spectra combined with the light intensity ($I^E_{i,j}$ and $I^F_{i,j}$) were the transmittance spectra. The distance between positions O and E was much larger than that between positions E and F. Therefore, the scattering of the solution was relatively weak, and the absorbance of the absorption layer ($A_{i,j}$) can be calculated by Eq. (2) and expressed approximately by Eq. (3).

D. Data processing

Previous studies show that partial least squares regression (PLSR) is an effective method to handle spectral data.[21]

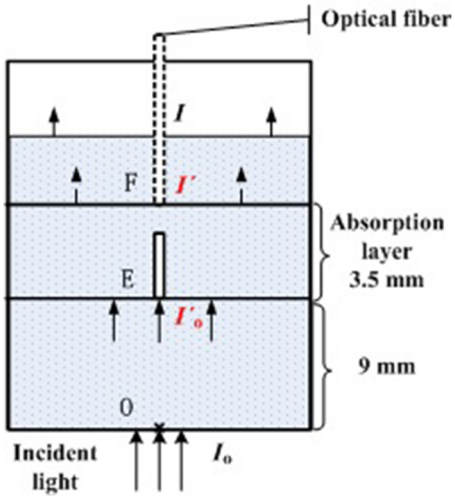

FIG. 3. Positions of spectral measurement in the experiment. (Positions E and F are the first and second measuring positions of the absorption layer, respectively.)

We selected the PLSR method as the modeling algorithm. The relationship between the transmittance spectra (or the absorbance spectra) and the concentration of the solution was established by modeling with the main fraction, n.

In order to evaluate the efficiency and prediction accuracy of the proposed ML method, the transmittance spectra method (TS method) was employed as the reference. The TS method is widely used in NIR spectral analysis, and its measurement accuracy is satisfactory. In this paper, I'_o (as shown in Fig. 3) was used as the transmittance intensity in the TS method and formed the modeling sets ($I^E_{i,j}$). The absorbance of the absorption layer in the ML method was calculated by Eq. (3), and the models were built with the absorbance ($A_{i,j}$). Intra-lipid concentrations were predicted by the models.

To evaluate the prediction accuracy, four schemes (as shown in Table I) were designed, and four methods were used to measure and calculate. Four groups of modeling sets were used corresponding to four methods: $S^{TS}_{i,j}$ represents modeling sets of the TS method, $S^{ML}_{i,j}$ represents modeling sets of the ML method, $S^{TS*}_{i,j}$ represents modeling sets of the TS* method, and $S^{ML*}_{i,j}$ represents modeling sets of the ML* method.

TABLE I. The different prediction schemes. i is one of the five conditions of the light intensity (L1, L2, L3, L4, L5) and j represents the concentration. $S^{TS}_{i,j}$: $S^{TS}_{i,j} = I^E_{i,j}$ are sets of the TS method. $S^{ML}_{i,j}$: $S^{ML}_{i,j} = A_{i,j}$ are samples of the ML method and $A_{i,j}$ is the absorbance.

Methods \ Schemes		1	2	3	4
	Calibration samples	Prediction samples			
TS	$S^{TS}_{5,j}$	$S^{TS}_{4,j}$	$S^{TS}_{3,j}$	$S^{TS}_{2,j}$	$S^{TS}_{1,j}$
ML	$S^{ML}_{5,j}$	$S^{ML}_{4,j}$	$S^{ML}_{3,j}$	$S^{ML}_{2,j}$	$S^{ML}_{1,j}$
TS*	$S^{TS*}_{5,j}$	$S^{TS*}_{4,j}$	$S^{TS*}_{3,j}$	$S^{TS*}_{2,j}$	$S^{TS*}_{1,j}$
ML*	$S^{ML*}_{5,j}$	$S^{ML*}_{4,j}$	$S^{ML*}_{3,j}$	$S^{ML*}_{2,j}$	$S^{ML*}_{1,j}$

The * symbol indicates that the data were processed with normalization before modeling. Modeling sets in the state of L5 (i = 5) were used as the calibration sets, i.e., $S^{TS}_{5,j}$, $S^{ML}_{5,j}$, $S^{TS*}_{5,j}$, $S^{ML*}_{5,j}$. The modeling sets in states of L4 (i = 4), L3 (i = 3), L2 (i = 2), and L1 (i = 1) were used as prediction sets.

The normalization algorithm employed in this paper is

$$q_k = Q_k / Q_{\max}, \tag{4}$$

where q_k is the normalized result, Q_k is the intensity or absorbance at the kth wavelength, and $Q_{\max}$ is the maximum of the intensity or absorbance at all wavelengths.

$S^{TS*}_{i,j}$: $S^{TS*}_{i,j} = I^E_{i,j}/I^E_{i,j\max}$ are modeling sets of the TS method after normalization processing, which were calculated with Eq. (4).
$S^{ML*}_{i,j}$: $S^{ML*}_{i,j} = A_{i,j}/A_{i,j\max}$ are modeling sets of the ML method after normalization processing, which were calculated with Eq. (4).
TS*: The samples are the normalized incident light intensities, and the model was established by the TS method.
ML*: The samples are the normalized absorbances, and the model was established by the ML method.

The performance of the ML method was evaluated in two stages. First, the effectiveness of the ML method was confirmed by comparing the prediction accuracy with that of the TS method. Second, the effect of eliminating the influence of incident light changes was observed.

The performance of models was assessed by using the principal component score (n), correlation coefficient of the calibration set (r^2_c), correlation coefficient of the prediction set (r^2_p), root mean square error of prediction (*RMSEP*), and root mean square error of calibration (*RMSEC*).

IV. RESULTS AND DISCUSSION

A. Results of experiments

The absorption wavelength of intra-lipids in the NIR region is in the range of 1040-1160 nm. The transmittance spectra of 20% intra-lipid solution with five incident light intensities are shown in Fig. 4, and the corresponding absorbance spectra of 20% intra-lipid solution are shown in Fig. 5. The transmittance spectra and the absorbance spectra of other concentrations were similar to those of 20% intra-lipid solution.

The modeling accuracies of the four methods are shown in Table II, and the prediction accuracies are shown in Table III. The label TS represents the processing results by the TS method, TS* represents the processing results by the TS method with the normalized incident light intensity as the modeling set, ML represents the processing results by the ML method, and ML* represents the processing results by the ML method with the normalized absorbance as the modeling sample. Since the calibration sample sets in all schemes consisted of spectral data in the case of L5, the accuracy parameters of the calibration model in all schemes were the same (as shown in Table II).

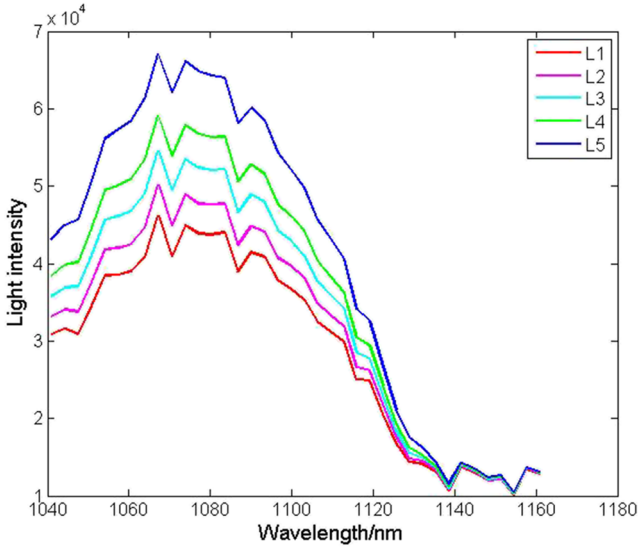

FIG. 4. Transmittance spectra of the 20% intra-lipid solution in five incident lights (L1, L2, L3, L4, and L5 represent five conditions of the incident light).

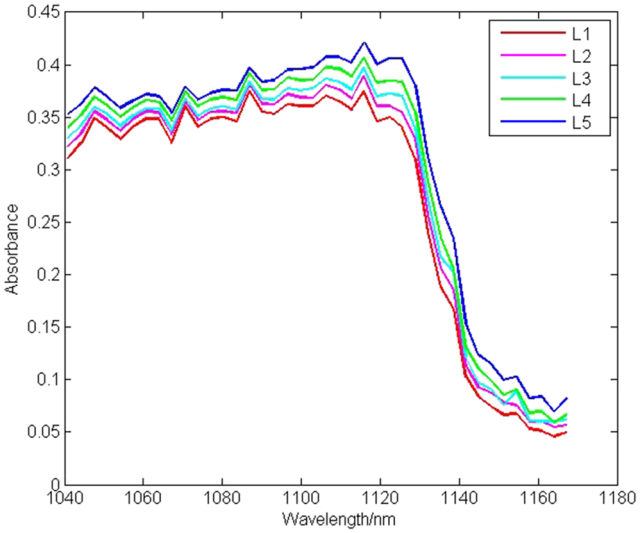

FIG. 5. Absorbance spectra of the 20% intra-lipid solution in five incident lights (L1, L2, L3, L4, and L5 represent five conditions of the incident light).

B. The influence of incident light variations

As shown in Fig. 4, as the incident light variations increased from 5.3% to 23%, the transmittance spectra increased by 39%-47.3%, and the absorbance spectra changed by 7.9%-13.5% (as shown in Fig. 5). These mean that the influence of the incident light changes on transmittance spectra was serious. The absorbance was also affected by the incident light variations but to a lesser degree than the transmitted light. Therefore, the ML method with absorbance spectra was superior to the TS method with transmission spectra.

TABLE II. Modeling accuracy of the four methods.

RMSEC				r_c^2		*n*	
TS	TS*	ML	ML*	TS	ML	TS	ML
0.536	0.082	0.513	0.181	0.994	0.995	3	3

TABLE III. Prediction accuracy of the four methods.

	RMSEP				r_p^2	
Schemes	TS	TS*	ML	ML*	TS	ML
1	1.975	1.225	0.987	0.647	0.994	0.994
2	3.727	2.558	1.572	1.255	0.993	0.988
3	5.288	3.958	3.036	1.572	0.990	0.990
4	7.007	5.711	4.219	2.148	0.988	0.986

C. The feasibility of ML method

Three main conclusions can be drawn from the results (as shown in Tables II and III): (i) all r_p^2 and r_c^2 were greater than 0.98, which indicate good correlation of the models; (ii) *RMSEC* values of the four methods were all less than 0.54, indicating that the training models were correct; (iii) *RMSEP* values of the ML method were 40%-57.8% smaller than those of the TS method, which means that the predictive accuracy of the ML method was higher than that of the TS method. All of the above results indicate that the ML method is feasible in spectral analysis. The biggest difference between the TS method and ML method is that the relationship between the modeling set and the composition of the solution is different.

Assuming that the incident light is constant, according to Lambert-Beer's law, the relationship between the transmittance spectra and the solution concentration is exponential ($I = I_0 e^{\varepsilon bc}$). When the incident light changes, the relationship would become complex and unpredictable, and the prediction ability of the model would worsen. This is an intractable issue of the TS method. As mentioned earlier, calibrating the incident light and processing with algorithms are commonly used to solve the problem. High cost and easy introduction of new errors are the disadvantages of these methods.

Other approaches, such as expanding the coverage of samples and collecting more samples in the original measurement range, are usually applied to solve the problem. These methods can improve the accuracy and robustness of the model, but a large increase in sample size may lead to high cost and longer measurement time. Moreover, problems still exist due to the changes in incident light generated by the difference between the modeling environment and the measurement environment.

The above-mentioned problems can be solved by the ML method. As the incident light and transmitted light of the absorption layer are measured, the absorbance represents their ratio and is independent of the incident light changes. The prediction ability of the model established by the ML method is insensitive to the incident light variations. Therefore, the ML method has the advantages of small sample size, short measurement time, and robustness.

D. The combination of ML method and normalization procedure

Usually, the effects of incident light variations are reduced by a normalization procedure. The modeling sets ($S_{i,j}^{TS*}$ and

$S_{i,j}^{ML*}$, as shown in Table II) were preprocessed with the normalization procedure. The results presented two main conclusions (as shown in Table III): (i) *RMSEP* of the TS* method was larger than that of the TS method and *RMSEP* of the ML* method was larger than that of the ML method. This indicates that after normalization processing, the prediction accuracy was increased. (ii) *RMSEP* of the TS method was much larger than that of the ML* method, especially when the incident light varied greatly (e.g., schemes 3 and 4). This result shows that the ML* method was much better than the TS method in eliminating the influence caused by the incident light variations.

As the model was established with absorbance and preprocessing with normalization, *RMSEP* values of ML* were far lower than those of the TS method. Therefore, the influence of errors caused by the incident light changes, scattering, and other factors can be significantly reduced by the combination of the ML method with normalization preprocessing. The model has very high accuracy and robustness, and the ML* method can be used in highly precise measurements.

V. CONCLUSIONS

An efficient method for NIR spectral analysis with high prediction accuracy and robustness was proposed in this paper. Using the method of measuring in layer (ML method), the incident light and the transmitted light were measured, and the exact absorbance was calculated. A high accuracy prediction model was built with the absorbance. Furthermore, the proposed ML method addressed the difficulties in measuring the original incident light. Incident light variations were simulated by changing the excitation voltage of the light source used in this study. The experimental results demonstrated that the ML method has higher prediction accuracy and better robustness compared to the transmittance spectral modeling method. Normalization and other preprocessing algorithms were used together with the ML method to achieve high precision analysis. The synthetic approach can be used for highly precise measurement of parameters in spectral analysis. Additionally, this method can be applied in measurement systems where the incident light is different from the modeling system.

ACKNOWLEDGMENTS

This study was supported by the Tianjin Application Basis & Front Technology Study Programs (No. 14JCZDJC33100).

[1]K. Maruo and Y. Yamada, "Near-infrared noninvasive blood glucose prediction without using multivariate analyses: Introduction of imaginary spectra due to scattering change in the skin," J. Biomed. Opt. **20**, 047003 (2015).
[2]M. S. Bergholt, W. Zheng, K. Lin, K. Y. Ho, M. Teh, and K. G. Yeoh, "Combining near-infrared-excited autofluorescence and Raman spectroscopy improves *in vivo* diagnosis of gastric cancer," Biosens. Bioelectron. **26**, 4104–4110 (2011).
[3]G. Bazar, R. Romvári, A. Szabó, T. Somogyi, V. Éles, and R. Tsenkova, "NIR detection of honey adulteration reveals differences in water spectral pattern," Food Chem. **194**, 873–880 (2016).
[4]S. Saranwong and S. Kawano, "System design for non-destructive near infrared analyses of chemical components and total aerobic bacteria count of raw milk," J. Near Infrared Spectrosc. **16**, 389 (2008).
[5]S. R. Delwiche and R. A. Graybosch, "Binary mixtures of waxy wheat and conventional wheat as measured by NIR reflectance," Talanta **146**, 496 (2016).
[6]M. Zude, M. Pflanz, L. Spinelli, C. Dosche, and A. Torricelli, J. Food Eng. **103**, 68 (2011).
[7]S. Macho and M. S. Larrechi, "Near-infrared spectroscopy and multivariate calibration for the quantitative determination of certain properties in the petrochemical industry," TrAC, Trends Anal. Chem. **21**, 799–806 (2002).
[8]B. Urbaniak and Z. J. Kokot, "Analysis of the factors that significantly influence the stability of fluoroquinolone–metal complexes," Anal. Chim. Acta **647**, 54–59 (2009).
[9]P. Phan, D. Highton, J. Lai, M. Smith, C. Elwell, and I. Tachtsidis, "Multichannel multi-distance broadband near-infrared spectroscopy system to measure the spatial response of cellular oxygen metabolism and tissue oxygenation," Biomed. Opt. Express **7**, 4424–4440 (2016).
[10]S. Zhang, L. Zhang, G. Li, and L. Lin, "Suppression of inter-device variation for component analysis of turbid liquids based on spatially resolved diffuse reflectance spectroscopy," Rev. Sci. Instrum. **88**, 033104 (2017).
[11]G. Li, Y. S. Luo, Z. Li, Z. Y. Li, and L. Lin, RSC Adv. **6**, 38849–38854 (2016).
[12]K. S. Abedin, M. Hyodo, and N. Onodera, "Active stabilization of a higher-order mode-locked fiber laser operating at a pulse-repetition rate of 154 GHz," Opt. Lett. **26**, 151–153 (2001).
[13]Y. Peng and R. Lu, "An improved multispectral imaging system for apple fruit firmness prediction," in *2005 ASAE Annual International Meeting Sponsored by ASAE Tampa Convention Center Tampa, Florida* (ASAE, 2005), Vol. 17, p. 056172.
[14]M. P. Tsvirko and A. G. Svetashev, "A calibration kit of fluorescent standards for the UV spectral range of 230–410 nm," Opt. Mater. **31**, 1842–1844 (2009).
[15]H. M. Hasanien, "FPGA implementation of adaptive ANN controller for speed regulation of permanent magnet stepper motor drives," Energy Convers. Manage. **52**, 1252–1257 (2011).
[16]B. Yu, L. F. Henry, and N. Ramanujam, "Instrument independent diffuse reflectance spectroscopy," J. Biomed. Opt. **16**, 011010 (2011).
[17]C. V. Greensill and K. B. Walsh, "Optimization of instrumentation precision and wavelength resolution for the performance of NIR calibrations of sucrose in a water-cellulose matrix," Appl. Spectrosc. **54**, 426–430 (2000).
[18]M. Zeaiter, J. M. Roger, and V. Bellon-Maurel, "Robustness of models developed by multivariate calibration. Part II: The influence of pre-processing methods," TrAC, Trends Anal. Chem. **24**, 437–445 (2005).
[19]X. Li and Y. He, "Discriminating varieties of tea plant based on Vis/NIR spectral characteristics and using artificial neural networks," Biosyst. Eng. **99**, 313–321 (2008).
[20]Q. Chen, J. Zhao, C. H. Fang, and D. Wang, "Feasibility study on identification of green, black and oolong teas using near-infrared reflectance spectroscopy based on support vector machine (SVM)," Spectrochim. Acta, Part A **66**, 568–574 (2007).
[21]I. V. Kovalenko, G. R. Rippke, and C. R. Hurburgh, "Determination of amino acid composition of soybeans (glycinemax) by near-infrared spectroscopy," J. Agric. Food Chem. **54**, 3485–3491 (2006).